

## Broadband shock-associated noise from a high-performance military aircraft

Aaron B. Vaughn, Tracianne B. Neilsen, Kent L. Gee, et al.

Citation: *The Journal of the Acoustical Society of America* **144**, EL242 (2018); doi: 10.1121/1.5055392

View online: <https://doi.org/10.1121/1.5055392>

View Table of Contents: <https://asa.scitation.org/toc/jas/144/3>

Published by the [Acoustical Society of America](#)

---

### ARTICLES YOU MAY BE INTERESTED IN

#### [Similarity spectra analysis of high-performance jet aircraft noise](#)

*The Journal of the Acoustical Society of America* **133**, 2116 (2013); <https://doi.org/10.1121/1.4792360>

#### [Source characterization of full-scale tactical jet noise from phased-array measurements](#)

*The Journal of the Acoustical Society of America* **146**, 665 (2019); <https://doi.org/10.1121/1.5118239>

#### [Summary of "Supersonic Jet and Rocket Noise"](#)

*Proceedings of Meetings on Acoustics* **31**, 040002 (2017); <https://doi.org/10.1121/2.0000655>

#### [Characterizing acoustic shocks in high-performance jet aircraft flyover noise](#)

*The Journal of the Acoustical Society of America* **143**, 1355 (2018); <https://doi.org/10.1121/1.5026026>

#### [Flow structure and acoustics of supersonic jets from conical convergent-divergent nozzles](#)

*Physics of Fluids* **23**, 116102 (2011); <https://doi.org/10.1063/1.3657824>

#### [Introduction to the special issue on supersonic jet noise](#)

*The Journal of the Acoustical Society of America* **151**, 806 (2022); <https://doi.org/10.1121/10.0009321>

---

**JASA**  
THE JOURNAL OF THE  
ACOUSTICAL SOCIETY OF AMERICA

**Special Issue:**  
**Additive Manufacturing and Acoustics**

Read Now!

# Broadband shock-associated noise from a high-performance military aircraft

**Aaron B. Vaughn, Tracianne B. Neilsen, and Kent L. Gee**

*Department of Physics and Astronomy, Brigham Young University, Provo, Utah 84602, USA*

*aaron.burton.vaughn@gmail.com, tbn@byu.edu, kentgee@byu.edu*

**Alan T. Wall**

*Air Force Research Laboratory, Battlespace Acoustics Branch, 2610 Seventh Street, Building 441, Wright-Patterson Air Force Base, Ohio 45433, USA*

*alan.wall.4@us.af.mil*

**J. Micah Downing and Michael M. James**

*Blue Ridge Research and Consulting, LCC, 29 North Market Street, Suite 700, Asheville, North Carolina 28801, USA*

*micah.downing@blueridgeresearch.com, michael.james@blueridgeresearch.com*

**Abstract:** Broadband shock-associated noise (BBSAN) is a prominent noise component from nonideally expanded jets in the forward and sideline directions. BBSAN from laboratory-scale jets has been studied extensively, and spatial trends in BBSAN spectral peak characteristics—frequency, level, and width—have been established. These laboratory-scale trends are compared to those for BBSAN from a tied-down F-35B operated at four engine conditions. While the peak frequency varies as expected, both spatially and across engine condition, the peak level and width do not, pointing to the need for additional research into BBSAN for high-performance military aircraft.

© 2018 Acoustical Society of America

[S-KL]

**Date Received:** June 22, 2018    **Date Accepted:** September 6, 2018

## 1. Introduction

The noise levels from high-performance military aircraft are a concern for communities near airbases, pilots, maintainers, and other personnel working with these aircraft. Therefore, models are being developed to appropriately predict the sound field of military aircraft. One important noise component is broadband shock-associated noise (BBSAN), which is prominent in the forward and sideline directions, as shown in Fig. 1. BBSAN was first studied by Harper-Bourne and Fisher<sup>1</sup> and has been primarily analyzed in laboratory-scale jets,<sup>2–11</sup> including a large series of tests at NASA Langley Research Center.<sup>5,6</sup> Only recently has BBSAN been investigated for a few locations near a tied-down, high-performance military aircraft operating at afterburner.<sup>12</sup> In this letter, a detailed analysis is presented of the spatial variation in BBSAN for a tied-down F-35B at different engine powers to explore if BBSAN from an installed high-performance aircraft engine exhibits the same features as in laboratory-scale jet noise studies.

There are two components of shock-associated noise in nonideally expanded supersonic jets: screech tones and BBSAN. Screech tones are harmonically related discrete tones that originate from an acoustic feedback loop between the first shock cell and the engine.<sup>1</sup> Screech tones are strong in underexpanded jet flow, while overexpanded jet flow—the case for an engine of a tied-down high-performance military aircraft—is essentially screech-free.<sup>13</sup> Present in both under and overexpanded jets, BBSAN originates from the weak interaction between downstream propagating large turbulent structures and the quasi-periodic shock cells in the jet plume.<sup>4</sup> For laboratory-scale jets, the primary BBSAN spectral peak has a distinctive shape that Pao and Seiner<sup>11</sup> show rises steeply with  $f^4$  below the peak frequency and decays as  $f^2$  at frequencies just above the peak.

In addition to this distinctive spectral shape, three parameters—frequency, level, and width—characterize the first BBSAN spectral peak. These parameters vary both spatially and with jet conditions, such as the jet speed, temperature, and whether the jet is over or underexpanded. In particular, the degree of mismatch between the design Mach number of the nozzle,  $M_d$ , and the jet Mach number,  $M_j$ , plays a large role. For the F-35B, however, the temperature and Mach numbers are unavailable and

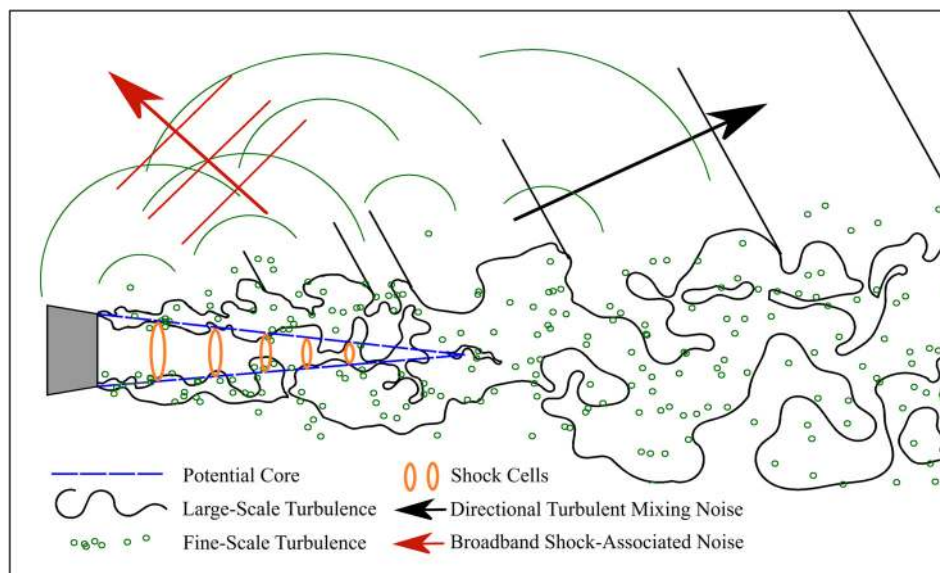


Fig. 1. (Color online) Schematic of jet noise with directional sound radiation of the large-scale turbulent mixing noise and the BBSAN indicated.

their relationship to the engine thrust request (ETR) is unknown. For nonideally expanded laboratory-scale jets, Tanna *et al.*<sup>2</sup> ascertained when the BBSAN contribution becomes more significant to the overall jet noise spectra (see Fig. 2 of Ref. 2). BBSAN levels rise as the mismatch between the jet and design Mach numbers ( $M_j$  and  $M_d$ , respectively) increases due to the increased strength of the shock cells. Notably, the BBSAN level changes as  $\beta^4$ , where  $\beta = \sqrt{(M_j^2 - M_d^2)}$  is referred to as the off-design parameter. BBSAN is more prominent than turbulent mixing noise at smaller inlet angles. As inlet angle increases, the turbulent mixing noise level increases dramatically and masks the BBSAN because the level of BBSAN is presumed to be relatively similar across angles.<sup>3</sup> BBSAN is more apparent at lower temperatures because turbulent mixing noise levels increase rapidly with increased temperature and, therefore, mask BBSAN over a wider angular aperture.<sup>2</sup>

For an overexpanded laboratory-scale jet, the three characterizing parameters of the main spectral peak of BBSAN exhibit consistent trends. Across the spatial aperture of a single jet noise measurement, BBSAN peak frequency increases with increased inlet angle (e.g., Fig. 10 of Ref. 2).<sup>2,10</sup> Conversely, the level decreases with inlet angle.<sup>2,9</sup> The width of the spectral peak broadens with increased inlet angle, as seen in Figs. 2–13 of Ref. 4. When comparing between jet noise measurements, as the off-design parameter increases, the BBSAN peak frequency decreases [see Fig. 17 of Ref. 3 and Fig. 11(a) of Ref. 2], the level increases, and the width becomes narrower.<sup>2,3</sup> As temperature increases, frequency decreases slightly (see Fig. 7 of Ref. 3 and Fig. 16 of Ref. 9), while the overall sound pressure level (OASPL) and level of the BBSAN spectral peak increase slightly and the width broadens.<sup>3,9</sup> However, temperature appears to have only a minimal affect that quickly saturates as the temperature increases.<sup>3</sup> As the off-design parameter and temperature are unavailable for the F-35B engine, the variation in the frequency, level and width of the F-35B BBSAN are analyzed as a function of inlet angle and ETR.

Recently, the first analysis of BBSAN from military aircraft engine was performed by Tam *et al.*<sup>12</sup> They reported spatial trends for these same three characteristics for a tied-down F/A-18E operating at afterburner. In agreement with the laboratory-scale case, the peak frequency of F/A-18E BBSAN was shown to increase with increasing inlet angle. However, the peak level increases and the width were reported to decrease with increasing inlet angle—opposite the laboratory-scale trends. Because these trends were defined across a limited number of locations and only one engine condition, further investigations are needed to characterize BBSAN in high-performance military aircraft noise.<sup>14</sup>

This letter characterizes the BBSAN from a tied-down F-35B operated at multiple engine conditions. A measurement description is followed by a detailed analysis of the spatial variation in the frequency, level, and width of the primary BBSAN spectral peak, as well as changes across the engine operating conditions that produced

BBSAN: 75%, 100%, 130%, and 150% ETR. Comparisons are made with laboratory-scale studies and the preliminary afterburning F/A-18E results in Ref. 12. Differences in the spatial variation in peak level and width indicate areas where research is needed to understand BBSAN production from high-performance military aircraft.

## 2. Experiment

Noise measured near an F-35B during a ground run-up test at Edwards Air Force Base<sup>15</sup> provides the opportunity to investigate how the BBSAN changes with angle and engine condition. National Instruments PXI-4498 cards sampling at 204.8 kHz were used to synchronously acquire 30-s acoustic pressure waveform data. During the measurements, the F-35B engine operated multiple times at seven ETRs: idle, 25%, 50%, 75%, 100% (military power), 130% (minimum afterburner), and 150% ETR (maximum afterburner). Level variations between 5 and 6 run-ups at each engine condition is less than  $\pm 1$  dB. At idle, 25%, and 50% ETR, BBSAN was not present. However, BBSAN is a dominant feature of the noise for 75% ETR and higher at inlet angles less than  $73^\circ$ .

Analysis of the spatial variation in BBSAN is facilitated by the linear array located approximately 8 m from the estimated jet shear layer (see Fig. 2). The 71 element, ground-based array of GRAS 6.35 mm ( $1/4$ " ) pressure microphones had 0.45 m inter-microphone spacing and spanned 32 m, covering an angular aperture of  $35^\circ$ – $152^\circ$ . Consistent with other full-scale jet noise studies,<sup>12,14,15</sup> angles are defined relative to the jet inlet and the microphone array reference point (MARP) at  $z = 7.5$  m. Therefore, some geometry is required to connect these full-scale studies with laboratory-scale jet noise studies that defined angles from the nozzle. The MARP is selected to be representative of the estimated maximum source location for turbulent mixing noise at the peak frequencies.<sup>16,17</sup> The apparent acoustic source region of the BBSAN is likely forward of the MARP and is currently being investigated with both beamforming and near-field acoustical holography.<sup>18</sup>

## 3. Results

The features of the F-35B BBSAN may be compared with trends seen in prior laboratory-scale jet studies. The BBSAN characteristics under investigation are the frequency, level, and width of the primary BBSAN spectral peak. The F-35B measurements allow for an investigation of the spatial variation of these characteristics at a single ETR, as well as changes across ETR. For each ETR at every microphone location, the power spectral density (PSD) with a 3 Hz resolution is computed, and the frequency ( $f_{\text{peak}}$ ), level ( $L_{\text{peak}}$ ), and bandwidth associated with the top 3 dB ( $\Delta_{3\text{dB}}$ ) of the BBSAN spectral peaks are identified. The  $L_{\text{peak}}$  are scaled to a common distance of 30 m from the MARP based on a spherical spreading assumption. (Nonlinear propagation effects have been identified at the small inlet angles associated with BBSAN for supersonic, imperfectly-expanded, heat-simulated model jets<sup>19</sup> and the F-35B measurements analyzed in this paper.<sup>20</sup> However, the primary BBSAN spectral peak occurs at frequencies considerably lower than those affected by nonlinear propagation over this short distance. Thus, the spherical spreading assumption is adequate for establishing spatial trends.)

The overall spectral shape of F-35B BBSAN is fairly consistent with the laboratory-scale studies. As an example, Fig. 3 shows the PSD at the smallest measured inlet angle,  $35^\circ$ , for 75% ETR (a) and 150% ETR (b). The BBSAN spectral peak has a sharp rise and a slightly less steep decay in most cases. Figure 3(a) shows that the spectral slopes of the F-35B BBSAN are close to the  $f^4$  and  $f^{-2}$  slopes described

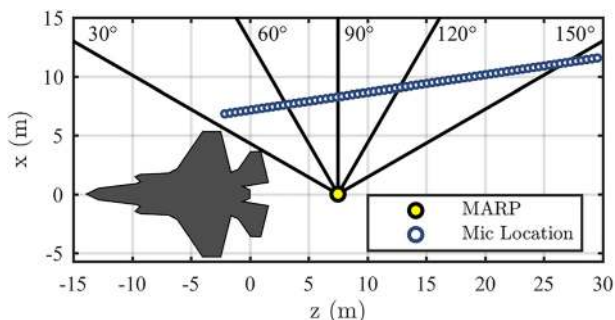


Fig. 2. (Color online) Measurement layout of the linear ground array near an F-35B. The microphone array reference point (MARP) and microphone locations are marked.

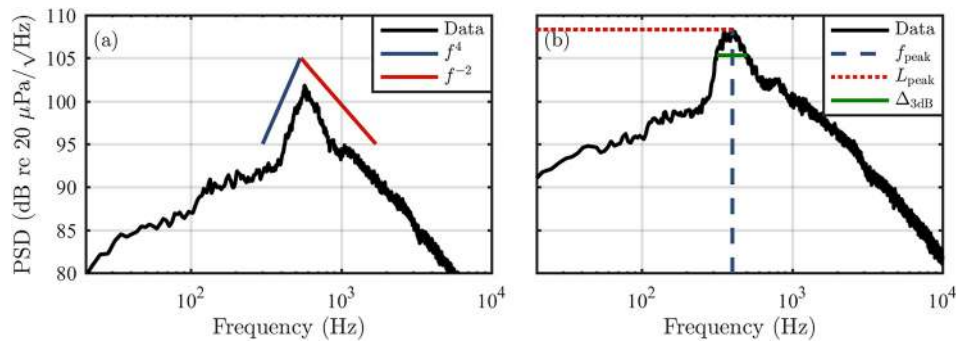


Fig. 3. (Color online) F-35B power spectral density (PSD) at 35° for (a) 75% ETR and (b) 150% ETR. Characteristic frequency slopes ( $f^4$  rise and  $f^{-2}$  decay) of BBSAN described by Pao and Seiner (Ref. 11) are shown in (a), and the primary BBSAN features are indicated in (b): peak level ( $L_{\text{peak}}$ ), peak frequency ( $f_{\text{peak}}$ ), and width of the spectral peak corresponding to the top 3 dB ( $\Delta_{3\text{dB}}$ )

by Pao and Seiner.<sup>11</sup> The F-35B BBSAN peak is more pronounced in the forward direction (small inlet angles) and becomes less distinguished as inlet angle increases due to the increase in turbulent mixing noise. The other features of the BBSAN spectral peak are labeled in Fig. 3(b).

The peak frequency of the BBSAN increases with inlet angle across all F-35B engine conditions, similar to laboratory-scale studies. The  $f_{\text{peak}}$ , shown in Fig. 4(a), is easily definable at small inlet angles. The lines in Fig. 4 represent the mean across the run-ups for a given engine condition, with dots showing the values for individual run-ups. The uncertainty in the exact value of  $f_{\text{peak}}$  increases towards the end of the angular aperture shown because the BBSAN spectral peak becomes broader due to the increased contribution of the turbulent mixing noise as inlet angle increases. With increased ETR, the BBSAN is identifiable over a slightly larger angular range, and therefore higher ETR cases have additional data points in Figs. 4(a) and 4(b). While the same trend over angle is evident at all engine conditions,  $f_{\text{peak}}$  is higher at 75% ETR than at 100% ETR and remains the same or decreases slightly for 130% and 150% ETR. This limited change for higher ETR is consistent with the saturation effect of increased beta and temperature shown for laboratory-scale jet in Fig. 12(b) of Ref. 3.

Unlike  $f_{\text{peak}}$ , the spatial variation in peak level of the F-35B BBSAN,  $L_{\text{peak}}$ , depicted in Fig. 4(b), differs from the laboratory-scale trend at higher ETR. At every location, the  $L_{\text{peak}}$  values are higher for larger ETR, which matches the increase in BBSAN seen in laboratory-scale jets as the temperature and off-design parameter increases. At 75% ETR, as inlet angle increases,  $L_{\text{peak}}$  decreases similar to laboratory-scale jets. At 100% ETR,  $L_{\text{peak}}$  remains relatively constant until 50° after which it begins to decrease, aside from an anomalous increase of about 1 dB at 64°, the cause of which is unknown. At 130% ETR, the  $L_{\text{peak}}$  values remain relatively constant, whereas at 150% ETR,  $L_{\text{peak}}$  increases approximately 2 dB between 35° and 48° then varies only slightly as inlet angle increases to 73°. (For the greatest inlet angles at which BBSAN is defined, the  $L_{\text{peak}}$  values are likely 1–2 dB higher than what should be attributed to BBSAN due to the incoherent addition of the turbulent mixing noise, which increases in level as inlet angle increases until it completely masks the BBSAN spectral peak.) The spatial trends at higher-ETR disagree with the result from a 2017 study<sup>12</sup> of BBSAN for a tied-down, afterburning F/A-18E of increasing peak level with inlet angle. The slight increase in level for the F-35B BBSAN at 150% ETR [Fig. 4(b)] does, however, agree with the BBSAN spectra for an uninstalled “supersonic jet engine at high set point” shown in Fig. 6(a) of Schlinker *et al.*,<sup>21</sup> indicating that this trend is not due to installation effects. Thus, the  $L_{\text{peak}}$  at 75% ETR follows the spatial trend observed in laboratory-scale jets, the higher ETRs do not.

The final BBSAN characteristic, the width of the first spectral peak, is quantified by finding the bandwidth over which the levels are within 3 dB ( $\Delta_{3\text{dB}}$ ) of the peak, as illustrated by the green lines in Fig. 3(b). Because the width relative to the peak frequency is of more importance, the resulting  $\Delta_{3\text{dB}}/f_{\text{peak}}$  are shown in Fig. 4(c). Similar trends across inlet angle are seen when a cutoff of 2 and 4 dB are used to define the widths. As the inlet angle increases, the turbulent mixing noise levels rise to a point where it affects the width of the spectral peak, such that  $\Delta_{3\text{dB}}$  is no longer a definable characteristic of the BBSAN. From observing the PSD plots, this interference is seen as  $\Delta_{3\text{dB}}/f_{\text{peak}}$  approaches 0.6 for 75% and 0.8 for 150% ETR. Hence, at some of the

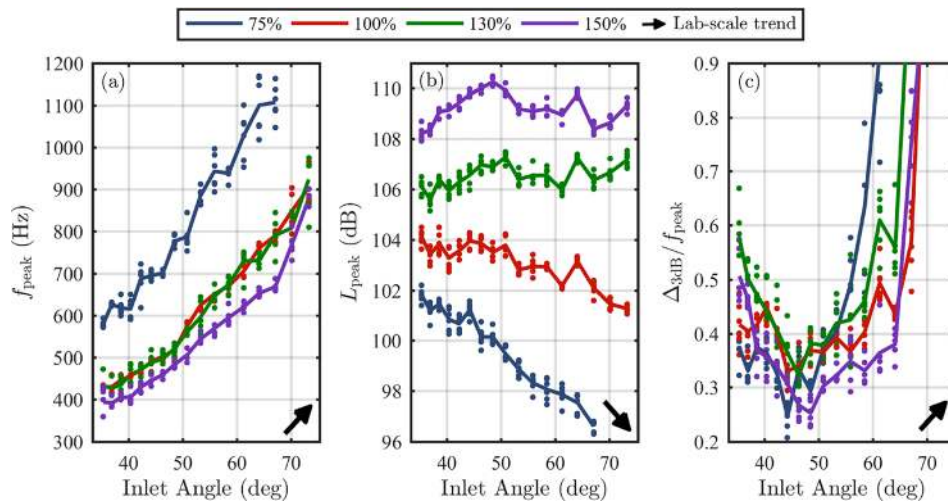


Fig. 4. (Color online) BBSAN characteristics across inlet angle for four F-35B engine conditions, given as percentage engine thrust request. (a) Peak frequency,  $f_{\text{peak}}$ ; (b) peak level,  $L_{\text{peak}}$ ; and (c) spectral width of the top 3 dB,  $\Delta_{3\text{dB}}$ , scaled by  $f_{\text{peak}}$ . Dots represent individual run-ups and solid lines denote the engine-condition average. Arrows in the lower right of each plot represent a general trend of increasing or decreasing with inlet angle observed in laboratory-scale studies, but the slope of the line is not to be interpreted quantitatively.

locations where  $f_{\text{peak}}$  and  $L_{\text{peak}}$  can be identified, the  $\Delta_{3\text{dB}}/f_{\text{peak}}$  is not shown, resulting in fewer data points in Fig. 4(c) than Figs. 4(a) or 4(b). The effect of the rising turbulent mixing noise can be seen in the rapid increase of the  $\Delta_{3\text{dB}}/f_{\text{peak}}$  values at the largest inlet angles shown at each ETR; the presence of the increasing turbulent mixing noise limits the accuracy of the width estimation as inlet angle increases.

At all four ETRs, the F-35B BBSAN scaled width decreases to some extent or remains relatively the same before increasing. Especially pronounced at 150% ETR, the change in  $\Delta_{3\text{dB}}/f_{\text{peak}}$  appears to be inversely related to the change in peak level: as the peak level increases/decreases, the BBSAN spectrum becomes narrower/wider. Without the dimensionless  $\Delta_{3\text{dB}}/f_{\text{peak}}$ , the  $\Delta_{3\text{dB}}$  appears to become narrower as ETR increases, yet relative to the peak frequency, the width of the BBSAN spectral peak represents approximately the same fraction of an octave for inlet angles up to  $55^\circ$ . The F-35B spatial trend for the width of the BBSAN to first decrease then increase with inlet angle differs from both the continual increase in width seen in laboratory-scale BBSAN and decreasing width identified for the BBSAN of a tied-down F/A-18E at afterburner from Ref. 12. These differences between laboratory and full-scale BBSAN and the BBSAN of two different high-performance military aircraft points to the need to investigate these spectral characteristics further. These investigations should include the possible relationship between BBSAN peak width and  $L_{\text{peak}}$  across angle and engine power, as seen with the F-35B data.

#### 4. Conclusion

This study of BBSAN from a tied-down F-35B provides a comprehensive look at how the BBSAN varies spatially and what changes result from an increase in ETR. The overall spectral shape of F-35B BBSAN at 75% to 150% ETR is fairly consistent with the laboratory-scale studies. Spatially, the BBSAN  $f_{\text{peak}}$  increases with inlet angle across all F-35B engine conditions, similar to laboratory-scale studies. The peak frequencies are lower at 100% than at 75% ETR, and peak frequencies at 130% and 150% ETR are similar to those at 100% ETR indicating a saturation of this effect. As observed with laboratory-scale BBSAN, the  $L_{\text{peak}}$  values at 75% ETR decrease with increased inlet angle. In addition,  $L_{\text{peak}}$  increases with ETR as expected. However, the angular variation of  $L_{\text{peak}}$  changes at higher ETRs. At 100% ETR, the  $L_{\text{peak}}$  remains rather constant before decreasing with inlet angle, while at 130% ETR, the  $L_{\text{peak}}$  remains relatively constant. At 150% ETR,  $L_{\text{peak}}$  increases slightly before decreasing as inlet angle increases. The variation in  $L_{\text{peak}}$  at 150% ETR is similar to that seen for an uninstalled engine.<sup>21</sup> For all engine conditions, the F-35B BBSAN spectral width unexpectedly decreases slightly or remains relatively constant before increasing, whereas the literature only predicts increasing width for laboratory-scale jets. This behavior appears linked to the variation in peak level. The cause for differences between the F-35B and laboratory-scale BBSAN need to be investigated, as does the apparent disagreement with BBSAN from an afterburning F/A-18A/E reported in Ref. 12. An improved

understanding of the relationship between the BBSAN characteristics and the engine power is needed to improve modeling of high-performance military aircraft noise.

### Acknowledgments

The authors gratefully acknowledge funding for the measurements, provided through the F-35 Program Office and Air Force Research Laboratory. Analysis was supported in part through a grant from the Office of Naval Research Grant No. N000141410494. A.B.V. thankfully recognizes an undergraduate research assistantship received from the College of Physical and Mathematical Sciences, Brigham Young University. (Distribution A: Approved for public release; distribution unlimited. F-35 PAO Cleared 05/16/2018; JSF18-529).

### References and links

- <sup>1</sup>M. Harper-Bourne and M. J. Fisher, “The noise from shock waves in supersonic jets,” *AGARD-CP-131*, 1–13 (1973).
- <sup>2</sup>H. K. Tanna, “An experimental study of jet noise part II: Shock associated noise,” *J. Sound Vib.* **50**(3), 429–444 (1977).
- <sup>3</sup>C. W. Kuo, D. K. McLaughlin, and P. J. Morris, “Effects of jet temperature on broadband shock-associated noise,” *AIAA J.* **53**, 1515–1530 (2015).
- <sup>4</sup>C. K. W. Tam, “Broadband shock associated noise of moderately imperfectly expanded supersonic jets,” *J. Sound Vib.* **140**, 55–71 (1990).
- <sup>5</sup>T. D. Norum and J. M. Seiner, “Broadband shock noise from supersonic jets,” *AIAA J.* **20**, 68–73 (1982).
- <sup>6</sup>J. M. Seiner and J. C. Yu, “Acoustic near-field properties associated with broadband shock noise,” *AIAA J.* **22**, 1207–1215 (1984).
- <sup>7</sup>P. K. Ray and S. K. Lele, “Sound generation by instability wave/shock-cell interaction in supersonic jets,” *J. Fluid Mech.* **587**, 173–215 (2007).
- <sup>8</sup>S. A. E. Miller, “The prediction of scattered broadband shock-associated noise,” *AIAA J.* **54**, 343–359 (2015).
- <sup>9</sup>K. Viswanathan, “Scaling laws and a method for identifying components of jet noise,” *AIAA J.* **44**, 2274–2285 (2006).
- <sup>10</sup>C. K. W. Tam and H. K. Tanna, “Shock associated noise of supersonic jets from convergent-divergent nozzles,” *J. Sound Vib.* **81**, 337–358 (1982).
- <sup>11</sup>S. P. Pao and J. M. Seiner, “Shock-associated noise in supersonic jets,” *AIAA J.* **21**, 687–693 (1983).
- <sup>12</sup>C. K. W. Tam, A. C. Aubert, J. T. Spyropoulos, and R. W. Powers, “On the dominant noise components of tactical aircraft: Laboratory to full scale,” AIAA Paper No. 2017-3516 (2017).
- <sup>13</sup>B. P. Petitjean, P. J. Morris, and D. K. McLaughlin, “On the nonlinear propagation of shock-associated jet noise,” AIAA Paper No. 2005-2930 (2005).
- <sup>14</sup>T. B. Neilsen, A. B. Vaughn, K. L. Gee, S. H. Swift, A. T. Wall, J. M. Downing, and M. M. James, “Inclusion of broadband shock-associated noise in spectral decomposition of noise from high-performance military aircraft,” AIAA Paper No. 2018-3146 (2018).
- <sup>15</sup>A. T. Wall, K. L. Gee, M. M. James, K. A. Bradley, S. A. McNerny, and T. B. Neilsen, “Near-field noise measurements of a high-performance military jet aircraft,” *Noise Control Eng. J.* **60**, 421–434 (2012).
- <sup>16</sup>A. T. Wall, K. L. Gee, T. B. Neilsen, R. L. McKinley, and M. M. James, “Military jet noise source imaging using multisource statistically optimized near-field acoustical holography,” *J. Acoust. Soc. Am.* **139**(4), 1938–1950 (2016).
- <sup>17</sup>T. A. Stout, K. L. Gee, T. B. Neilsen, A. T. Wall, and M. M. James, “Source characterization of full-scale jet noise using acoustic intensity,” *Noise Control Eng. J.* **63**, 522–536 (2015).
- <sup>18</sup>K. M. Leete, A. T. Wall, K. L. Gee, T. B. Neilsen, M. M. James, and J. M. Downing, “Dependence of high-performance military aircraft noise on frequency and engine power,” AIAA Paper No. 2018-2826 (2018).
- <sup>19</sup>B. P. Petitjean, K. Viswanathan, and D. K. McLaughlin, “Acoustic pressure waveforms measured in high speed jet noise experiencing nonlinear propagation,” *Int. J. Aeroacoust.* **5**, 193–215 (2006).
- <sup>20</sup>B. O. Reichman, K. L. Gee, T. B. Neilsen, S. H. Swift, A. T. Wall, H. L. Gallagher, J. M. Downing, and M. M. James, “Acoustic shock formation in noise propagation during ground run-up operations of military aircraft,” AIAA Paper No. 2017-4043 (2017).
- <sup>21</sup>R. H. Schlinker, S. A. Liljenberg, D. R. Polak, K. A. Post, C. T. Chipman, and A. M. Stern, “Supersonic jet noise source characteristics & propagation: Engine and model scale,” AIAA Paper No. 2007-3623 (2007).